Journal of Aerosol Science 120 (2018) 62–81

Contents lists available at ScienceDirect

Journal of Aerosol Science

journal homepage: www.elsevier.com/locate/jaerosci

CFD Simulation of aerosol particle removal by water spray in the model containment THAI

C. Kaltenbach*, E. Laurien

Institute of Nuclear Energy and Energy Systems (IKE), University of Stuttgart, Pfaffenwaldring 31, 70569 Stuttgart, Germany

ARTICLE INFO

Keywords:
Two-phase flow
Containment flow
THAI
CFD
Aerosol
Spray

ABSTRACT

A spray system in the upper containment part of a PWR (Pressurized Water Reactor) is an effective mitigation mechanism to reduce the spread of radioactive particles inside the reactor building. Radioactive particles and hot water steam can be released out of a leak in the primary circuit during a severe accident. CFD (Computational Fluid Dynamics) simulation of spray is a challenging task in the field of nuclear reactor safety. To use commerical codes like ANSYS CFX for flow analysis in nuclear reactor safety, user defined physical models must be implemented to investigate relevant thermohydraulic physical phenomena like heat and mass transfer between droplets and the atmosphere. In the current publication a CFD model is presented, which is able to describe the extraction of aerosol particles in an atmosphere by water spray. The model is applied in ANSYS CFX16.1 and is compared to experimental data of AW4, which was performed in the German model containment THAI (Thermal-hydraulics, Hydrogen, Aerosols and Iodine). During the experiment, a spray is injected into THAI to reduce the particle content in an aerosol atmosphere. Particle concentrations at different measure planes in THAI are used for comparison with simulations. Simulations use different droplet and particle size groups (mono- and poly-disperse) in a full three dimensional geometrical mesh of THAI. Each size class is modeled by a seperate velocity field.

1. Introduction

During a severe accident in a PWR (Pressurized Water Reactor), hot water vapor and radioactive core particles can be released into the containment building. To reduce the thermal and mechanical stresses on the containment structure and to washout the particle contamination, a spray nozzle system which is mounted in the upper containment part, injects cold water into the heated and particle saturated atmosphere. Spray systems contribute to the efficiency of the reactor safety concept, e.g. in the EPR (European Pressurized Water Reactor, see Kessler et al. (2014).

There are only a few publications in the literature concerning particle washout with spray in the nuclear field. Experimental investigations concerning the removal behavior of aerosol particles in the field of nuclear reactor safety were first done in the French TOSQAN model containment by IRSN, e.g. Porcheron and Lemaitre (2008). They pressurized TOSQAN with a hot gas atmosphere which contains silicon carbide (SiC) as aerosol particles and injected a cold water spray through a nozzle to remove them. The spray injection significantly reduces the SiC content in the TOSQAN atmosphere. Marchand, Porcheron, Lemaitre, and Grehan (2006) developed a physical model for particle removal by spray. The model considers mechanical and phoretic removal effects when spray droplets interact with particles. The physical model was implemented in the Lumped-Parameter Code ASTEC and was applied to an

* Corresponding author.
E-mail address: christian.kaltenbach@ike.uni-stuttgart.de (C. Kaltenbach).

https://doi.org/10.1016/j.jaerosci.2018.03.005
Received 10 October 2017; Received in revised form 2 January 2018; Accepted 29 March 2018
Available online 31 March 2018
0021-8502/

Nomenclature

Greek

α	volume fraction,[-]
ρ	phase averaged density, [kg/m^3]
Γ	mass source term, [kg/m^3 s]
η	single droplet removal efficiency,[-]
μ	dynamic viscosity,[Ns/m^2]
σ	dynamic viscosity ratio,[-]
τ	response time, [s]
$\underline{\underline{\tau}}$	molecular stress tensor, [N/m^2]
$\underline{\underline{\tau}}^{Re}$	turbulent Reynolds stresses, [N/m^2]

Latin

c	mass fraction, [-]
c $_D$	drag coefficient,[-]
d	diameter,[m]
d $_{32}$	Sauter diameter, [m]
D	diffusion coefficient, [m^2/s]
g	gravity, [m/s^2]
J	empirical factor ,[-]
K	empirical factor,[-]
M	momentum source term,[N/m^3 s]
$\overline{p}$	absolute pressure, [bar]
Pe	Peclet number, [-]
R	diameter ratio, [-]
Re	Reynolds number, [-]
s	drop height, [m]
S *	correction factor, [-]
Sc	Schmidt number, [-]
St	Stokes number, [-]
t	time, [s]
$\overrightarrow{u}$	phase averaged velocity vector,[m/s]
$\dot{V}$	volumetric flow rate of spray,[m^3/s]
V $_{con}$	containment volume,[m^3]

Index

Air	air
all	summation of all removal processes
CsI	caesium iodine
dyn	dynamic
D	drag force
Diff	Brownian diffusion
G	gas phase
H2O	water
imp	inertial impaction
int	interception
k	phase indicator
L	liquid phase
m	x,y,z-coordinates
P	particle phase
T	turbulent

aerosol spray washout experiment, which was conducted in TOSQAN. In addition to, experimental investigations were done in the German model containment THAI. Several experiments, which cover a wide range of accident scenarios with aerosol particle release, were performed. A broad overview of the conducted experiments is given by Gupta et al. (2015). One of the performed experiments, namely AW4, is used in the current publication for validation. Theoretical work concerning aerosol particle removal in simple test cases like tube flows was done by Jung and Lee (1998) and Park, Jung, Jung, Lee, and Lee (2005).

To use the advantages like detailed investigations of flow fields and the first principle approach of CFD in the field of nuclear reactor safety, commercial codes like ANSYS CFX16.1 need specific thermohydraulic physical models for heat and mass transfer, which must be implemented via user defined functions. Normally, commercial codes do not have special physical models for nuclear application. This paper presents a model, which is able to predict the particle removal behavior of a water spray, which is injected into a particle laden gas atmosphere. We consider mechanical mechanisms like settling, inertial impaction, interception and Brownian diffusion and compare the simulations to experimental data of THAI AW4. CFD simulations are conducted with monodisperse and polydisperse size groups for droplets and particles. Moreover, the present two-fluid model is extended to a three-fluid approach, where particles possess their own velocity field. The washout model is not restricted to soluble or non-soluble particles, since the resolution from a solid to a liquid particle inside of droplets is not considered. A physical description of the resolution process solid/liquid is combinable with the current washout model.

2. Numerical model

2.1. Euler-Euler two-fluid approach

The presented model and simulations are based on the Euler-Euler two-fluid approach, which was introduced by Ishii and Mishima (1984) and Ishii and Hibiki (2006). Each physical condition (liquid, gas) is represented by a single phase. All participating phases are continuous and interpenetrating each other all over the flow domain. To determine the phases, the volume fraction α_k is introduced. Index k is the phase indicator and stands for liquid (L) or gas (G). The continuous gas phase is considered as air. Air is a simplified mixture regarding 79% nitrogen and 21% oxygen, noble gases and other minor gas species are neglected. Droplets consist of water and can be described continuously with an assumption of spherical shape. Interactions between phases (mass, momentum and energy transfer) are taken into account with source and sink terms in the conservation equations.

The conservation equations are presented below. All simulations are done isothermal, therefore the energy conservation equation is not considered. Mass conservation is described by

$$\frac{\partial \alpha_k \rho_k}{\partial t} + \nabla\left(\alpha_k \rho_k \overrightarrow{\overline{u}}^k\right) = \Gamma_k. \tag{1}$$

ρ_k and $\overrightarrow{\overline{u}}^k$ represent the phase averaged density and the velocity vector of phase k. t is the physical time and Γ_k stands for the source or sink term of mass, which is modeled for aerosol particle removal in the current publication. Due to simplifications in the two-fluid approach, the gas phase is treated as a variable mixture of air and small aerosol particles. Small particles are treated as species of the gas phase, therefore air and particles share the same velocity field (slip behavior between gas and particles is neglected) and computational effort is reduced, see Kaltenbach and Laurien (2017). This simplification is only valid for small particles, in the current case approximately 1 μm. An aerosol is a mixture of a carrier gas and small suspended particles. Important for the physical behavior of an aerosol is the ability of particles (Index P) to follow the carrier gas in case of an abrupt change of direction, e.g. the flow around an obstacle. The capability of a particle to follow the carrier gas is dependent on the density ratio between gas ρ_G and particle ρ_P and the ratio between the diameter of the aerosol particle d_P and the obstacle (here: droplet d_L). Fig. 1 a shows the flow around a droplet with a small particle.

The streamline of the particle (red dashed line) is similar to that of the gas phase (black solid line). When both streamlines are compared for larger particles, see Fig. 1 b), a discrepancy is obvious. Both, the carrier gas and the particle move on their own trajectory. To assess, whether particle and carrier gas share the same velocity field or not, the Stokes number St can be consulted. St is the ratio between the dynamic response time τ_{dyn} of a particle reacting on a velocity change and a characteristic response time of the carrier flow τ_G. We can describe St according to Crowe, Sommerfeld, and Tsuji (1998)

$$St = \frac{\tau_{dyn}}{\tau_G} = \frac{\rho_P \cdot d_P^2 \cdot \overline{u}^G}{18 \cdot \mu_G \cdot d_L}. \tag{2}$$

In eq. (2), μ_G stands for the dynamic viscosity of the gas phase. If St is far below 1, a good agreement between the particle and the gas streamline can be assumed. For St equal to 1 or greater, particles must be described with their own velocity field, since there is an influence of particles on gas and vice versa. Due to the use of small monodisperse particles of approximately 1 μm in the current two-fluid approach according to the validation experiment, St is far below 1 in all of the two-fluid simulations and therefore gas and particles are modeled in a single velocity field neglecting momentum transfer between gas and aerosol particles.

For the assumption of particles as part of the gas phase, mass balance equations for air and particles must be solved. The validation experiment AW4 uses caesiumiodine as particles, so the particles are shortened with the index CsI in the mass balance equations

$$\frac{\partial(\alpha_G \rho_G c_{Air}^G)}{\partial t} + \nabla\left(\alpha_G \rho_G c_{Air}^G \overrightarrow{\overline{u}}^G\right) + \nabla(\alpha_G \rho_G D_T \nabla c_{Air}^G) = 0, \tag{3}$$

$$\frac{\partial(\alpha_G \rho_G c_{CsI}^G)}{\partial t} + \nabla\left(\alpha_G \rho_G c_{CsI}^G \overrightarrow{\overline{u}}^G\right) + \nabla(\alpha_G \rho_G D_T \nabla c_{CsI}^G) = \Gamma_G. \tag{4}$$

c_{Air}^G and c_{CsI}^G are the mass fractions of air and CsI, whereas D_T represents the turbulent diffusion, which is calculated with the turbulent Schmidt number $Sc_T = 0.9$. During spray injection, spray is responsible for a highly turbulent flow in the THAI gas atmosphere and therefore the molecular diffusion process is neglected in the simulations. Eq. (4) has a sink term observing the removed particles in the gas.

Beside the gas phase, a variable mixture is applied to droplets. The liquid phase consists of pure water (H_2O) and CsI particles. During the washout process, particles are transfered from the gas to the liquid phase. With a mixture approach for droplets, it is possible to model particle accumulation inside the droplet phase. Due to the variable mixture approach, mass balance equations for

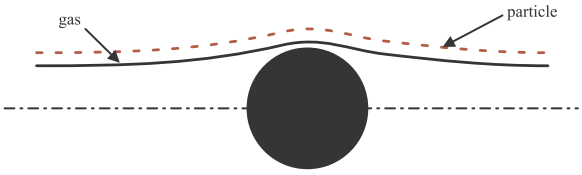

(a) Flow around a droplet for small particles

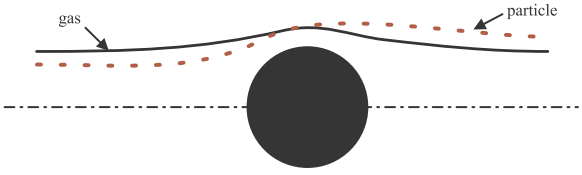

(b) Flow around a droplet for large particles

Fig. 1. Flow behavior around a droplet for small and large particles.

the liquid phase must be considered,

$$\frac{\partial(\alpha_L \rho_L c^L_{H_2O})}{\partial t} + \nabla\left(\alpha_L \rho_L c^L_{H_2O} \overline{\vec{u}}^L\right) = 0, \tag{5}$$

$$\frac{\partial(\alpha_L \rho_L c^L_{CsI})}{\partial t} + \nabla\left(\alpha_L \rho_L c^L_{CsI} \overline{\vec{u}}^L\right) = \Gamma_L. \tag{6}$$

In Eqs. (5) and (6), $c^L_{H_2O}$ and c^L_{CsI} are the mass fractions of H_2O and CsI in the droplet mixture. Diffusion is neglected in the droplet phase due to high droplet velocities and therefore a mass fraction transfer only because of convection. Turbulent diffusion is also neglected due to disperse consideration of the droplet phase and the assumption of a laminar flow for droplets. The maximum amount of CsI, which droplets can incorporate, is restricted to experimental data.

Momentum conservation for phase k in m-directions is represented by

$$\frac{\partial(\alpha_k \rho_k \overline{u}^k_m)}{\partial t} + \nabla\left(\alpha_k \rho_k \overline{\vec{u}}^k \overline{u}^k_m\right) = -\alpha_k \frac{\partial \overline{p}}{\partial x_m} + \nabla[\alpha_k(\underline{\underline{\tau}}^k + \underline{\underline{\tau}}^{Re,k})]_m + \overline{u}^k_m \Gamma_k + \alpha_k \rho_k g_m + M_{k,m}. \tag{7}$$

In eq. (7), $\overline{p}$ stands for the absolute pressure, $\underline{\underline{\tau}}^k$ and $\underline{\underline{\tau}}^{Re,k}$ observe the molecular and the turbulent Reynolds stresses, g_m is the gravitational force and $M_{k,m}$ is the source/sink term for momentum transfer between the liquid and the gas phase. Both phases use the same pressure field $\overline{p}$ due to a single pressure assumption and therefore the interfacial pressure and interfacial shear force are neglected.

There are different secondary conditions in the two-fluid approach, which have to be satisfied. Volume fractions α_k of all phases k have to sum to one everywhere in the flow domain and all modeled mass source/sink terms Γ_k have to yield zero

$$\alpha_L + \alpha_G = 1, \tag{8}$$

$$\Gamma_L + \Gamma_G = 0. \tag{9}$$

The turbulent Reynolds stresses $\underline{\underline{\tau}}^{Re,k}$ for the gas phase are modeled with the Shear Stress Turbulence (SST) model introduced by Menter (1994).

2.2. Extension of the Euler-Euler two-fluid approach towards a three-fluid approach

To investigate the influence of floating aerosol particles in THAI, a third velocity field must be introduced. Fig. 2 shows the distribution of velocity fields in a two-fluid (a) and a three-fluid approach (b).

The two-fluid approach represents one liquid (mixture of H_2O and CsI particles) and one gas (mixture of air and CsI particles) phase. Gas and particles as a mixture is valid for small particles, a mathematical assessment of this assumption is done later in Section 3. To take into account the particle dynamics especially for larger particles as supposed in the two-fluid approach, a third velocity field is necessary. In case of a three-fluid approach, k stands for L (liquid), G (gas) and P (particle). The equations described in Eqs. (1) and (7) are applied to all three phases. The gas phase is now modeled only with air, therefore mass balance equations for the gas phase are not applied. To investigate the influence of different droplet and particle sizes, the three-fluid approach is extended, see Fig. 3. Droplets and particles are segmented to take into account different size groups (from 1 to n size groups). Each size group of particle and droplet has a seperate velocity field with a complete set of conservation equations for mass and momentum.

Each particle and droplet size group is characterized by a constant droplet diameter. Source/sink terms for the particle washout is applied to each particle and droplet size group. Breakup and coalescence between the size groups is not observed neither in the particle phase nor in the droplet phase. Due to the focus on the particle removal process in the current work, interaction between particles can be neglected, since particles interact quickly with water droplets during spray activation. Coalescence or breakup of particles is important when particles move slowly in hardly moving gas atmospheres.

The secondary conditions for a three-fluid approach have to be extended with the additional particle phase as follows

$$\alpha_L + \alpha_G + \alpha_P = 1, \tag{10}$$

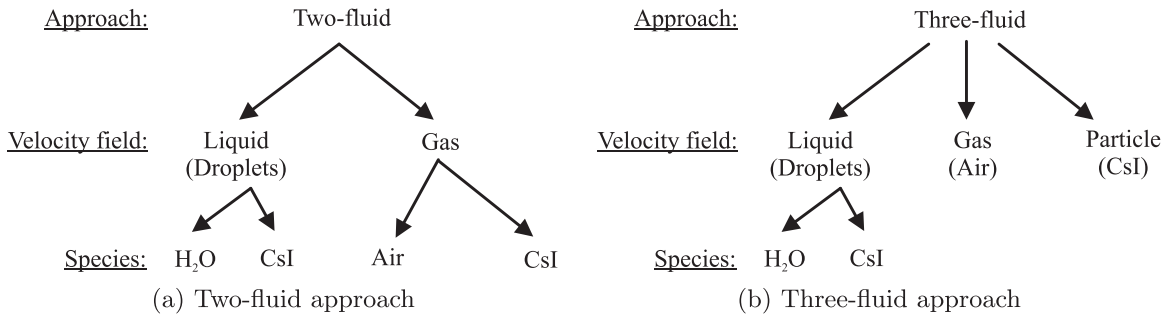

Fig. 2. Distribution of velocity fields in a two-fluid a) and a three-fluid approach b).

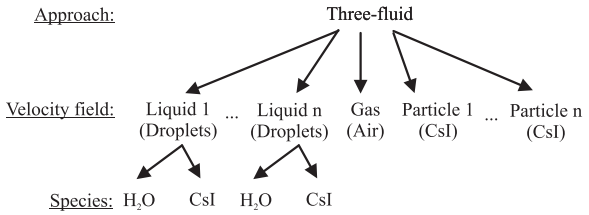

Fig. 3. Segmentation of three-fluid approach with different droplet and particle size classes.

$$\Gamma_L + \Gamma_P = 0. \tag{11}$$

2.3. Modeling of water droplets and aerosol particles

Both, droplets and aerosol particles are treated as small isolated spheres. In the following, the momentum interaction between gas/droplets and gas/particles is introduced

$$M_{G,m} = M^{D}_{G,m} = M^{D,LG}_{G,m} + M^{D,PG}_{G,m}. \tag{12}$$

$M_{G,m}$ is the total amount of momentum, which is exchanged between gas/droplets and gas/particles. In the current model only drag forces are considered, therefore $M_{G,m}$ is equal to $M^{D}_{G,m}$. Superscript D stands for drag. $M^{D}_{G,m}$ is represented by the drag force between gas/droplet $M^{D,LG}_{G,m}$ and gas/aerosol particle $M^{D,PG}_{G,m}$. Additional forces like the Basset force or the virtual mass force are neglected due to $\rho_L \gg \rho_G$ respectively $\rho_P \gg \rho_G$. The drag force between droplets and gas is described with the following equation

$$M^{D,LG}_{G,m} = -M^{D,LG}_{L,m} = \alpha_L \cdot \frac{3\rho_G}{4d_L} \cdot c_{D,LG} \cdot \left|\vec{\overline{u}}^{L} - \vec{\overline{u}}^{G}\right| \left(\vec{\overline{u}}^{L} - \vec{\overline{u}}^{G}\right). \tag{13}$$

d_L stands for the droplet diameter. According to Schiller and Naumann (Crowe et al., 1998), the drag coefficient $c_{D,LG}$ around a sphere is indicated with

$$c_{D,LG} = \frac{24}{Re^{LG}} \cdot (1 + 0.15 \cdot (Re^{LG})^{0.687}). \tag{14}$$

In eq. (14), the relative Reynolds number Re^{LG} is calculated using the velocity difference of the droplet and gas phase

$$Re^{LG} = \frac{\rho_G \cdot \left|\vec{\overline{u}}^{L} - \vec{\overline{u}}^{G}\right| \cdot d_L}{\mu_G}. \tag{15}$$

μ_G represents the dynamic gas viscosity. The drag force between aerosol particles and gas is modeled in the same way, nevertheless some variables must be swapped. Summarizing, the following equations are used

$$M^{D,PG}_{G,m} = -M^{D,PG}_{L,m} = \alpha_P \cdot \frac{3\rho_G}{4d_P} \cdot c_{D,PG} \cdot \left|\vec{\overline{u}}^{P} - \vec{\overline{u}}^{G}\right| \left(\vec{\overline{u}}^{P} - \vec{\overline{u}}^{G}\right), \tag{16}$$

$$c_{D,PG} = \frac{24}{Re^{PG}} \cdot (1 + 0.15 \cdot (Re^{PG})^{0.687}), \tag{17}$$

$$Re^{PG} = \frac{\rho_G \cdot \left|\vec{\overline{u}}^{P} - \vec{\overline{u}}^{G}\right| \cdot d_P}{\mu_G}. \tag{18}$$

The drag force definition is applied to all size groups of particles and droplets. In the two-fluid approach, momentum exchange between gas and aerosol particles is neglected due to negligence of slip behavior between air and particles. In this case $M^{D,PG}_{G,m}$ in eq. (12) is zero.

3. Modeling of aerosol particle removal by spray

There are different effects, which affect the particle removal behavior by water spray. Parsly (1971) and Marchand et al. (2006) subdivide the mechanisms in three parts:

- Negligible small flow velocity (settling)
- Mechanical effects (inertial impaction, interception, Brownian diffusion)
- Phoretic effects (thermophoresis, diffusiophoresis)

All mechanisms used in the current model to describe the behavior between droplets and aerosol particles are presented in the following subsections.

Important for the mathematical description of each removal mechanism is the single droplet removal efficiency η. Fig. 4 shows a single droplet, which moves in an envelope created through its downward movement.

Inside this envelope volume, plenty of aerosol particles exist. η describes the ratio between the particle mass collected by a single droplet and the particle mass present in the volume of the droplet trajectory and which may be collected by a single droplet. η can be defined with

$$\eta = \frac{\text{Particle mass collected in a single droplet}}{\text{Overall mass of particles in the trajectory volume}} \quad . \tag{19}$$

The correlations for the different mechanisms are completely independent from each other. To combine the removal efficiency of each mechanism to an overall removal efficiency for a single droplet η_{all}, the following correlation according to Strauss (1975) is used

$$\eta_{all} = 1 - (1 - \eta_{imp})\cdot(1 - \eta_{int})\cdot(1 - \eta_{Diff}). \tag{20}$$

η_{all} is dimensionless and can vary from zero to one. In eq. (20), η_{imp}, η_{int} and η_{Diff} are the single droplet removal efficiency for inertial impaction, interception and Brownian diffusion. η_{all} ensures a maximum removal efficiency of one. In case of a simple add up of η_{imp}, η_{int} and η_{Diff}, an unphysical removal efficiency larger than one is possible.

In the current work, simulations with the Euler-Euler two-fluid approach consider inertial impaction, interception and Brownian diffusion. Additionally to the previous mentioned effects, the Euler-Euler three-fluid model observes settling of particles in gas. In consequence of the density difference, particles are accelerated by the gravity and move towards the lower THAI plenum. The terminal velocity can be derived from force equilibrium around an aerosol particle, where the gravity force is equal to the drag force of the particle in a surrounding gas atmosphere. When we assume Stokes flow for a particle in gas, the terminal velocity $\overline{u}^P$ of a particle can be described by

$$\overline{u}^P = \frac{1}{18}\cdot\frac{1}{\mu_G}\cdot d_P^2\cdot\rho_P\cdot g. \tag{21}$$

For the considered flow configuration (monodisperse $d_P = 1.76\ \mu m$ and $\rho_P = 4500\ \mathrm{kg/m^3}$), $\overline{u}^P$ can be calculated to 0.00018 m/s. To confirm this assessment and to investigate the influence of larger aerosol particles and polydisperse particle configurations with $d_P > 1\ \mu m$, the Euler-Euler three-fluid approach is used.

η_{all} contains all relevant removal mechanisms for a single droplet. For mass conservation in eq. (1), a source and sink term is needed. The single droplet removal efficiency has to be scaled up to a complete spray, which consists of millions of small water droplets. Parsly (1971) suggests a removal source term Γ for the mass conservation and calculates a theoretical number of droplets the spray contains. Important information for the calculation are the volumetric spray flow rate, the drop height and the droplet diameter. Regarding the movement of a single droplet from injection at the nozzle to the sump of THAI, a wash out volume of this droplet can be determined. The wash out volume multiplied with total number of droplets injected lead to a total washout volume. To describe the removal source term Γ of particles, the total washout volume must be multiplied with ρ_L and η_{all}.

Γ in Eq. (22) is applied to the gas and the liquid phase in the Euler-Euler two-fluid approach in

$$\Gamma_L = -\Gamma_G = \frac{3\cdot\dot{V}\cdot s\cdot\rho_L}{2\cdot d_L\cdot V_{con}}\cdot\eta_{all}. \tag{22}$$

The three-fluid approach uses

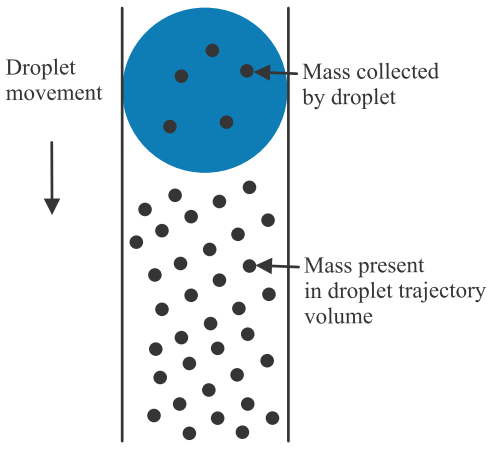

Fig. 4. Definition of the single droplet removal efficiency η.

$$\Gamma_L = -\Gamma_P = \frac{3 \cdot \dot{V} \cdot s \cdot \rho_L}{2 \cdot d_L \cdot V_{con}} \cdot \eta_{all}, \tag{23}$$

where the particles are modeled in a separate phase. In Eqs. (22) and (23), $\dot{V}$ is the volumetric flow rate of spray in the injection nozzle, V_{con} is the containment volume of THAI and s is the drop height. s describes the distance of the droplet falling through the aerosol atmosphere from the inject nozzle to the sump of THAI. In the current THAI configuration s is constant with a value of 7.4 m since the droplet nozzle is mounted 7.4 m above the sump (lowest level).

3.1. Inertial impaction

Hard collisions between droplets and particles are described as inertial impaction. Fig. 5 shows a moving droplet and its trajectory (dotdashed line) towards a particle. When the droplet hits the particle, the particle is removed from the gas atmosphere.

Seinfeld and Pandis (2006) defined a mathematical correlation for the single droplet removal efficiency η_{imp} due to inertial impaction

$$\eta_{imp} = \left[\frac{St - S^*}{St - S^* + 0.66} \right]^{\frac{3}{2}} \tag{24}$$

$$\text{with} \quad S^* = \frac{1.2 + \frac{1}{12} \cdot ln(1 + Re_{imp})}{1 + ln(1 + Re_{imp})} \tag{25}$$

$$\text{and} \quad Re_{imp} = \frac{d_L \cdot \overline{u}^L \cdot \rho_G}{\mu_G}. \tag{26}$$

S^* is an empirical correction factor and Re_{imp} is the specified Reynolds number for the gas phase. This effect is the most efficient one in the current application.

3.2. Interception

Like inertial impaction, interception considers contact between aerosol particles and droplets. Here, the contact is considered when a particle moves around a droplet and touches its surface. Through the contact, particles stick on the droplet surface and will be removed of the gas atmosphere. In Fig. 6, the dashed line represents the particle streamline flowing around the droplet and the dotdashed line expresses the streamline of the particle.

The single droplet removal efficiency for interception η_{int} can be modeled according to Park et al. (2005)

$$\eta_{int} = \frac{1 - a_L}{J + \sigma \cdot K} \cdot \left\{ \left(\frac{R}{1 + R} \right) + \frac{1}{2} \left(\frac{R}{1 + R} \right)^2 \cdot (3\sigma + 4) \right\} \tag{27}$$

$$\text{with} \quad J = 1 - \frac{6}{5} \cdot \alpha^{\frac{1}{3}} + \frac{1}{5} \cdot \alpha_L^2 \tag{28}$$

$$\text{with} \quad K = 1 - \frac{9}{5} \cdot \alpha^{\frac{1}{3}} + \frac{1}{5} \cdot \alpha_L^2 \tag{29}$$

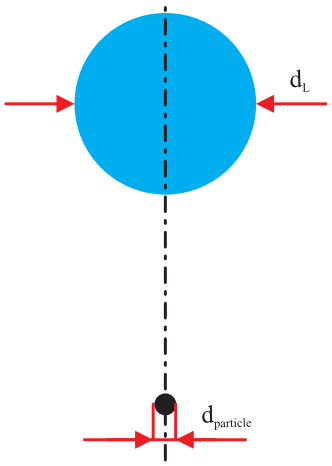

Fig. 5. Droplet and aerosol particle during inertial impaction.

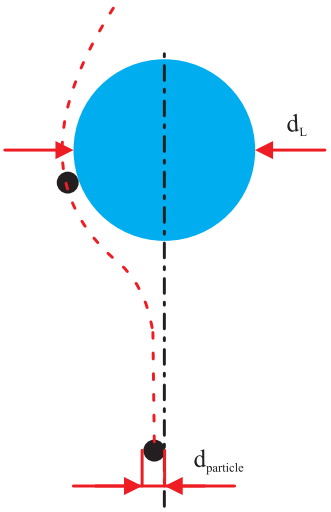

Fig. 6. Droplet and aerosol particle during interception.

$$\text{with} \quad \sigma = \frac{\mu_L}{\mu_G} \tag{30}$$

$$\text{and} \quad R = \frac{d_P}{d_L}. \tag{31}$$

J and K are empirical factors, which depend on α_L. σ is the ratio between the dynamic viscosity of the droplets μ_L and the gas phase μ_G and R is the ratio between particle diameter d_P and droplet diameter d_L.

3.3. Brownian diffusion

For aerosol particles smaller than 1 μm, Brownian diffusion can be important for the removal process, see Licht (1980). Gas molecules move due to thermal induced oscillations and owing to impinging of molecules on particles, momentum is transfered to the particles. In Fig. 7, a droplet (blue), gas molecules (red) and particles (black) are shown.

The single droplet removal efficiency η_{Diff} due to diffusion can be observed according to Johnstone and Roberts Licht (1980) with

$$\eta_{Diff} = \frac{4}{Pe} \cdot \left(2 + 0.557 \cdot Re_{imp}^{\frac{1}{2}} \cdot Sc^{\frac{3}{8}}\right) \tag{32}$$

$$\text{with} \quad Pe = Sc \cdot Re_{imp} \tag{33}$$

$$\text{and} \quad Sc = \frac{\mu_G}{\rho_G \cdot D}. \tag{34}$$

The correlation is dependent on the Peclet number Pe, Reynolds number Re_{imp} and the Schmidt number Sc.

4. Validation experiment THAI AW4

The experiment AW 4 (Schmidt, Colombet, Freitag, Gupta, & von Laufenberg, 2015), which is used for validation of the presented washout model, was conducted in the German model containment THAI, see Fig. 8 a).

THAI is a cylindrical vessel with hemispherical heads and a cylindrical sump with a height of 9.2 m, a diamter of 3.2 m and a volume of 60 m^3. Walls can be heated or cooled with a closed thermal oil system. A full cone spray nozzle, which can be characterized

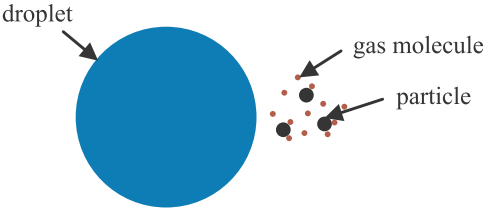

Fig. 7. Droplet and aerosol particle during diffusion.

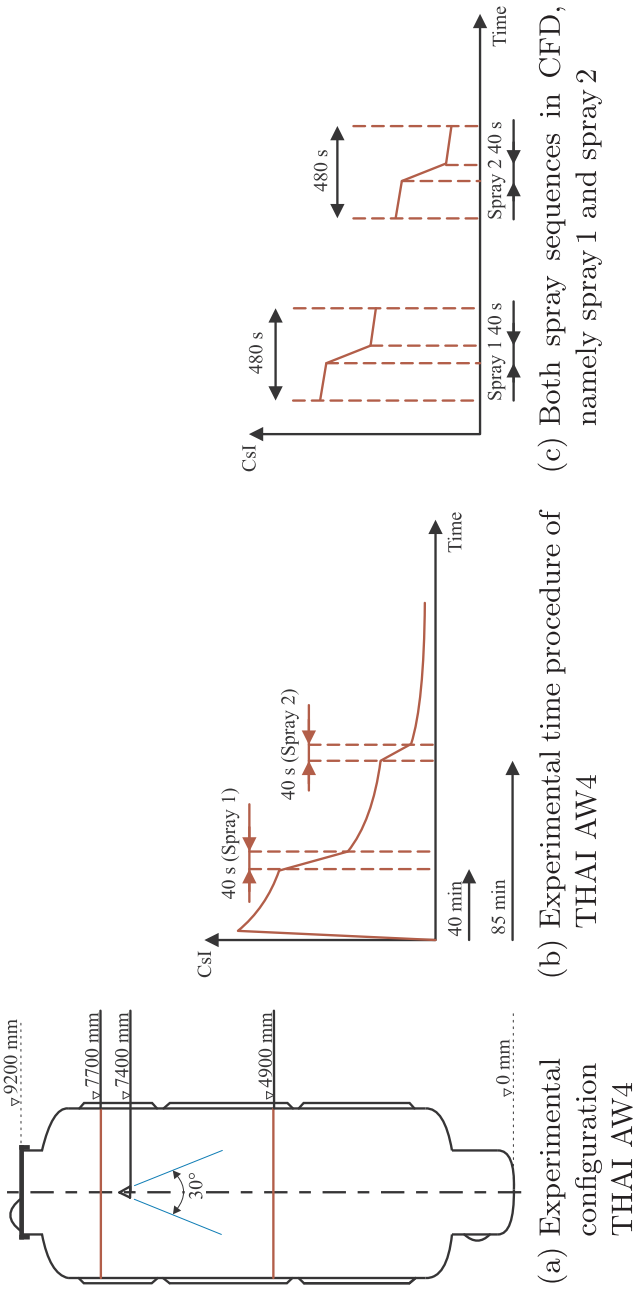

(a) Experimental configuration THAI AW4 (b) Experimental time procedure of THAI AW4 (c) Both spray sequences in CFD, namely spray 1 and spray 2

Fig. 8. THAI AW 4 configuration a) and time procedures (experimental and simulation) in b) and c).

with a Sauter-diamter of d_{32} = 830 μm and a spray angle of 30°, is used. The spray nozzle has an outlet diamter of 8 mm. Before the spray injection starts with a water mass flow rate of 1 kg/s, 0.2 kg Caesiumiodine (CsI) is injected in THAI and the containment is pressurized up to 1.5 bar. After CsI injection, the experiment assumes an uniform distribution of aerosol particles in the containment. Spray is activated twice for 40 s after 40 min and 85 min after CsI injection, see Fig. 8 b). Due to the idle time of 40 min until the first spray sequence will start and the associated settling process, the CsI content is transformed to a particle stratification with a higher particle content in the lower THAI area compared to the above located nozzle area. Between the first and the second spray sequence the same settling process is ongoing and reduces the CsI content in the upper THAI part. The simulations in the current work consider 4 min before spray activation and approximately 4 min after, which leads to a 480 s transient simulation, see Fig. 8 c. To consider stratified CsI content at the beginning of the both spray sequences, linear distributions are assumed based on measured CsI concentrations on two measure planes. The first plane is located at 7.7 m up from the THAI sump and plane two is at 4.9 m. Laser extinction (photometer) is used for the CsI measurements, which uses shading of the laser beam due to particles to conclude on the actual CsI concentration at the measure plane. The following presented linear distributions in Eqs. (35) and (36) define the particle content at the beginning of the simulations. Both numerical value equations calculate the CsI content in kg/m^3 and are dependend of the height coordinate z of THAI in meter. z = 0 m is in the axis of rotation in the sump of THAI.

$$\text{Spray1:} \quad \text{CsI} = -5.36\cdot10^{-5}\cdot z + 9.62\cdot10^{-4} \tag{35}$$

$$\text{Spray2:} \quad \text{CsI} = -1.07\cdot10^{-5}\cdot z + 3.32\cdot10^{-4} \tag{36}$$

During the first spray the mean value for d_P is 1.76 μm. For the second sequence d_P is 1.19 μm. This are mean values of d_P. An experimental particle size distribution, determined with impactors, are also used in the simulations. The mass fractions and associated particle sizes are presented in Tables 4, 5. Validation is done with CsI data gained on two measure planes. The first plane is located at 7.7 m up from the THAI sump and plane two is at 4.9 m.

Unfortunately there are no information given by the experimenters about uncertainties in the measurements. Therefore no statement can be made about the influence of the measurement equipment and the repeatability on the experiment.

5. CFD mesh and setup

All simulations are carried out in a full 360° 3D model of THAI. The applied unstructured mesh comprises one single flow domain and was created in ANSYS Meshing. It consists of approximately eight million tetrahedral volume elements. Fig. 9 a) presents a schematically resolution of the mesh in THAI and Fig. 9 b) near the injection nozzle. The mesh neglects wall structures, that means only the fluid domain is considered in the mesh neglecting the solid structure of THAI and nozzle walls. A higher concentration of tetrahedral elements in the nozzle region ensures a reasonable resolution of the spray injection area. Near the outer THAI wall,

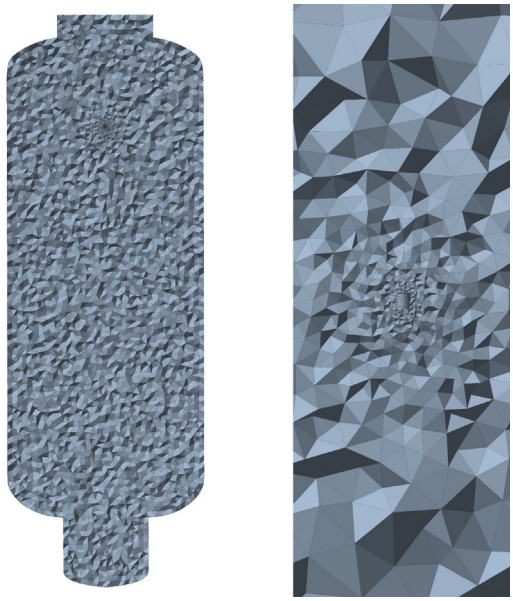

(a) Schematic grid resolution in THAI

(b) Grid resolution of THAI in the nozzle region

Fig. 9. Tetrahedral grid overall of THAI and near the spray nozzle.

automatic wall functions are used ($y^+ \gg 1$) to describe the boundary layer.

A sensivity study concerning the grid resolution in THAI was done with three meshes. All results of the study are presented in Section 6.5. In Table 1 meshes used in the sensivity study are shown.

Simulations are carried out with the commercial CFD code ANSYS CFX 16.1. The commercial CFD solver uses high resolution for the advection scheme and a second order backward Euler approach for the transient terms, 10^{-4} is set as convergence criteria. Simulations are done isothermal with a constant temperature of 90 °C and a constant absolute pressure of 1.5 bar. The accumulation of water droplets in the closed THAI vessel is not modeled in the simulations. Droplets disappear when touching THAI walls, this is achieved in the simulations using a sink term for droplets at the THAI walls. The current work is focussed on the droplet/particle interaction and therefore this approach reduces additional numerical effort. According to the experimental data, a linear CsI distribution at both test sequences is assumed before spray activation, see Eqs. (35) and (36). The experiment shows an increase of CsI towards the sump area. Spray droplets are able to absorb the removed CsI from the gas atmosphere. The droplet enrichment with CsI is restricted to the experiment, the absorption of CsI in the droplets was measured. At the spray nozzle, atomization from a continuous water flow to droplets is neglected, see Mimouni, Lamy, Lavieville, Guieu, and Martin (2010) and Malet, Huang et al. (2015). Droplet shape is assumed direct at the spray nozzle. Inlet velocity conditions for the spray are modeled by a velocity profile due to less experimental data. Unfortunately the experimental data for the spray velocity was measured only in the center point 15 cm below the spray outlet. The measurements for the full cone nozzle were done on the CALIST test station at the IRSN (Institut de Radioprotection et de Sûreté Nucléaire), see Malet and Mimouni (2015). Due to a lack of velocity information, the vertical velocity component u_Z over the whole nozzle outlet was assumed constant, see Fig. 10. The horizontal velocity components u_X and u_Y were calculated with a trigonometrical function depended on the spray angle. The angle ϕ was assumed with a linear distribution from the nozzle center (0°) to the edge of the nozzle (15°). Table 2 summarizes the values for the velocity components.

Simulations are carried out using the Euler-Euler two-fluid and three-fluid approach. The two-fluid simulations are done in two configurations

- Monodisperse droplets and monodisperse aerosol particles (Mono Mono 2Fl) ,
- Polydisperse droplets and monodisperse aerosol particles (Poly Mono 2Fl) .

The abbreviations of the configurations are shown in brackets. The first word represents the size distribution of the droplet phase, monodisperse (Mono) or polydisperse (Poly). The second part of the shortcut describes the configuration of the aerosol particles in the same way. '2FL' stands for the use of the Euler-Euler two-fluid model. Three-fluid simulations '3FL' use the following configurations

- Monodisperse droplets and monodisperse aerosol particles (Mono Mono 3Fl) ,
- Monodisperse droplets and polydisperse aerosol particles (Mono Poly 3Fl) ,
- Polydisperse droplets and polydisperse aerosol particles (Poly Poly 3Fl) .

Monodisperse droplet simulations are done with a Sauter-diameter d_{32} of 830 μm in both spray sequences. In the sequence of spray 1 with monodisperse aerosol particles, CsI is represented by a diameter of 1.76 μm. Spray 2 uses a diameter of 1.19 μm for particles in the monodisperse configuration. The diameter specification is according to the AW4 documentation in Langer and Colombet (2014). Polydisperse spray distributions use five different droplet size groups, see Table 3. Each droplet group is modeled as seperate single liquid fluid with a constant diameter and its own velocity field. Coalescence and breakup of droplets are neglected, all liquid volume fractions at the nozzle inlet are added up to one.

The polydisperse aerosol particle configurations use six different size classes. Tables 4, 5 show particle diameters and the mass fraction based on the overall particle mass of each particle size in spray 1 and spray 2. All used size classes were determined in the THAI AW4 experiment with impactors.

6. Results

6.1. Qualitative removal process

In the following, the aerosol particle washout with spray is shown qualitatively. For both spray sequences in the CFD simulations (spray 1 and spray 2), the flow field in THAI can be subdivided in three time dependend parts. The first part until 240 s indicates the flow field before spray activation. Part 2 from 240 s till 280 s shows the mechanical removal of aerosol particles and the third part is

Table 1
Mesh resolution used in the sensitivity study.

Mesh	Tetrahedral elements
Mesh 1	3.174.210
Mesh 2	8.163.746
Mesh 3	19.317.801

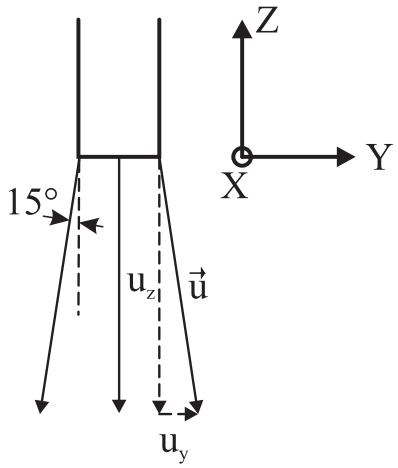

Fig. 10. Spray nozzle velocity distribution.

Table 2
Velocity components at spray nozzle inlet.

Component	Value
u_X	$tan(\phi) \cdot 23\,m/s$
u_Y	$tan(\phi) \cdot 23\,m/s$
u_Z	$-23\,m/s$

Table 3
Size classes of polydisperse spray.

Droplet class of mean size [mm]	Inlet volume fraction [%]
0.139	20
0.415	27
0.691	22
0.967	17
1.243	14

Table 4
Size classes of polydisperse aerosol particles in spray 1.

Particle class	Particle diameter [μm]	Mass fraction [%]
CsI 1	0.18	1
CsI 2	0.42	2
CsI 3	0.85	5
CsI 4	1.75	23
CsI 5	3.30	41
CsI 6	6.80	28

Table 5
Size classes of polydisperse aerosol particles in spray 2.

Particle class	Particle diameter [μm]	Mass fraction [%]
CsI 1	0.18	3
CsI 2	0.42	5
CsI 3	0.85	20
CsI 4	1.75	38
CsI 5	3.30	22
CsI 6	6.80	12

characterized by a homogenization of the CsI content in an abating gas flow in THAI without spray. For convenience, spray 1 is used below to explain the qualitative washout process. At the beginning of spray 1, aerosol particles in THAI are distributed according to experimental data, see Fig. 11 a). CsI concentration, which is measured in kg/m^3, is higher in the lower plenum than in the upper area. Spray activation after 240 s for 40 s leads to a massive reduction of the CsI content. The washout process is shown in detail in Fig. 11 c) - f). At 245 s, the removal process starts with a massive particle decrease in the spray center. The gas flow is redirected in

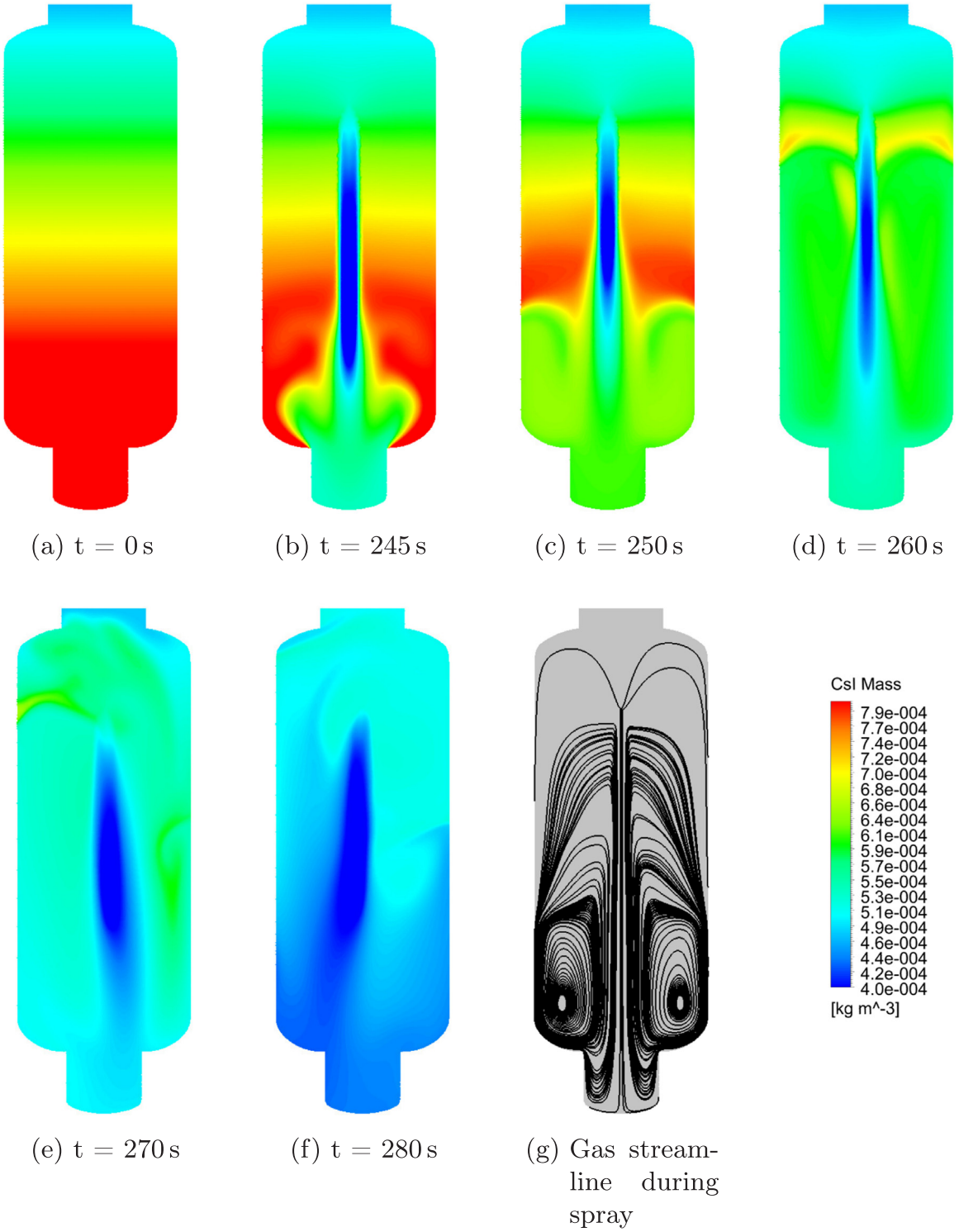

Fig. 11. CsI distribution during spray activation in spray 1 at different time steps.

the sump area and moves upward along the THAI wall. At 250 s, 260 s, 270 s and 280 s the washout process continues and drecreases the CsI content in THAI steadily and increases the CsI in the droplet phase, see Fig. 12 a and b). Fig. 11 g) shows the gas flow streamline during spray activation. Gas is entrained by drag between gas and droplets. The circulation gas flow in the lower containment part leads to a constant load of gas with high particle content to the washout area. The particle laden gas flow is sucked into the washout area at the height the spray nozzle is installed. At the end of spray activation, a slightly higher CsI distribution in the upper containment part is determined, see Fig. 11 f). The qualitative illustration of the washout process shows a highly three dimensional behavior during spray activation in THAI. When the droplet removal efficiencies of the removal mechanisms are compared to each other, inertial impaction is the most effective followed by interception and Brownian diffusion. Droplets are injected with a high velocity of approximately 23 m/s and lead to a highly turbulent flow in THAI. Droplets move towards particles with a high relative velocity which supports the removal by inertial impation and interception. Brownian diffusion has very little influence in the current removal process due to a very small amount of aerosol particles smaller than 1 µm, see Tables 4, 5.

Fig. 13 indicates the CsI distribution after spray activation is stopped. The flow field is still highly three dimensional and differences in CsI concentration in different areas are homogenized due to abating gas flow velocity. Though spray is stopped abruptly, gas remains in motion and decreases slightly because of friction on THAI walls and friction between gas molecules. The gas streamline is shown in Fig. 13 c).

6.2. Results gained with two-fluid approach

In Fig. 14, experimental data for CsI (y-axis) at the measure planes at 4.9 m and 7.7 m are compard to simulations using the Euler-Euler two-fluid approach with a mono-/polydisperse droplet and monodisperse particle configuration. The x-axis shows the time up to 480 s. Spray activation is between 240 s and 280 s. The plots illustrate three datasets, namely experiment (Exp), monodisperse simulation (Mono Mono 2Fl) and polydisperse (Poly Mono 2Fl). Fig. 14 c) and d) show an acceptable agreement for simulation and experiment in spray 2 after spray activation t > 280 s. Especially the polydisperse spray configuration shows a good agreement. When spray 1 is compared to the experiment, a different behavior is obvious. Here, the monodisperse droplet configuration shows a much better agreement than the polydisperse. One possible reason for the reduced efficiency of the removal process of the polydisperse spray configuration could be the reduced amount of larger droplets in the spray. When the droplet size classes of the polydisperse configuration (Table 3) are compared to d_{32} of the monodisperse spray, most of the droplets are smaller than d_{32}. Due to a smaller amount of large droplets in the polydisperse configuration, the washout efficiency is reduced. 69% of all droplets in the present polydisperse configuration are smaller than d_{32}. Simulations done with a smaller monodisperse droplet diameter than d_{32} confirm this phenomena, see Fig. 14 e) and f). Here, a fictional $d_L = 0.2$ mm is used in the same CFD setup d_{32} is using. A decreased d_L reduces the washout efficiency of droplets at both measure planes.

The aerosol particle diameter d_P in both sprays is monodisperse, in spray 1 d_P is 1.76 μm, in spray 2 d_P is 1.19 μm. For smaller particles the influence of a smaller amount of larger droplets is less important and therefore the results could be improved. The monodisperse spray configuration uses the same d_{32} in spray 2 and due to the large monodisperse droplets the removal efficiency is predicted too effective.

When the experimental spray part between 240 s and 280 s is compard to the simulations, discrepancies can be obtained.

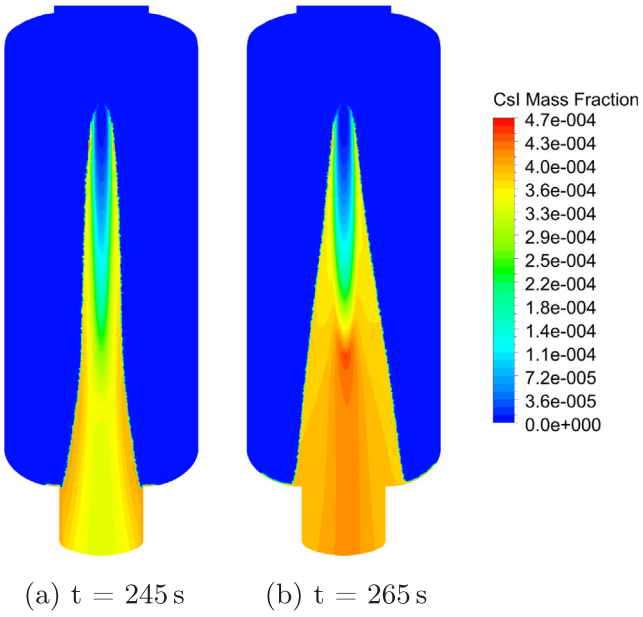

Fig. 12. CsI distribution inside of spray droplets at different time steps.

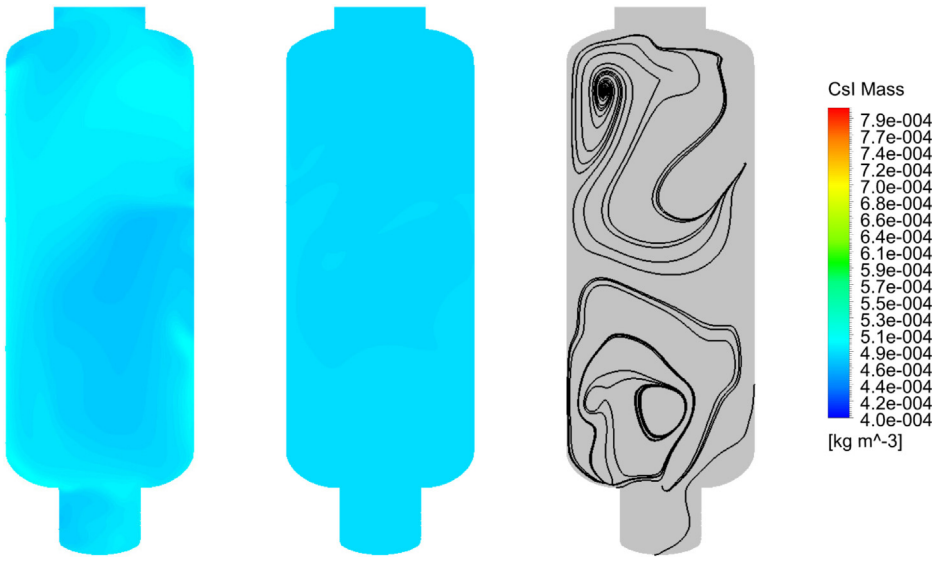

Fig. 13. CsI distribution in the third sequence at different time steps.

Especially at measure plane 4.9 m no agreement is obvious. Experimental data increase and the simulated ones decrease. This behavior can be explained by the measure principle of the CsI particles in THAI. The laser beam of the photometer, which is injected in THAI and penetrates the particle laden gas atmosphere, is detected via a diode. The intensity of the laser beam depends on aerosol particles moving through the beam. When droplets pass the beam, the intensity is additionally decreased because droplets are also detected as particles and therefore the CsI content is incorrectly increased. This fact causes the long simulation transient of 480 s with a part before and after spray activation, otherwise a comparison between experiment and simulation is not possible for measure plane 4.9 m.

Both spray configurations show a strong deviation in Fig. 14 b) from experimental data, especially the polydisperse spray. A reason for this behavior is the restriction to model only mechanical removal effects like inertial impaction etc., which become important when droplets interact with particles. In the period before and after spray injection (< 240 s and > 280 s), these mechanisms are not existing due to the missing spray. In these periods, for example settling effects get important. In the presented simulations in Fig. 14, the particles are treated as a species of the gas phase and therefore they share the same velocity field like air, neglecting a seperate particle velocity field. The missing degree of freedom in this approach prevents particles from settle down to the sump area although a much higher particle density is considered ($\rho_P = 4500\ \mathrm{kg/m^3}$) in comparison to air. This is the reason, why the CsI content remains constant before spray. After spray was injected and a fraction of CsI was washed out by droplets, the CsI content remains also constant. Spray injection homogenized the CsI distribution in the whole THAI facility. Settling out of this homogenized distribution is also not possible with a shared velocity field. The influence of a separate velocity field especially for particles is discussed in Section 6.4. Another restriction of the simulations is the negligence of wall effects. Particles can be trapped by wall roughness and wall friction. During spray, this is assumed to be negligible due to a high washout efficiency of droplets. In quiet flows without spray, this effects must be modeled.

6.3. Comparison of two-fluid and three-fluid approach for spray 1

Small particles can be handled as a species of the gas phase neglecting a seperate velocity field for particles. This approach was theoretically assessed for small particles in the current publication. In this section, the same spray and particle configuration is applied to a two-fluid and a three-fluid approach. Fig. 15 shows the comparison of a two (2FL) and three-fluid (3Fl) approach for spray 1.

For small monosized aerosol particles ($d_P = 1.76\ \mu m$) in spray 1, there is no difference between the different approaches at measure plane 4.9 m and 7.7 m. Both plots show nearly a perfect coincidence. The agreement confirms the theoretical assessment.

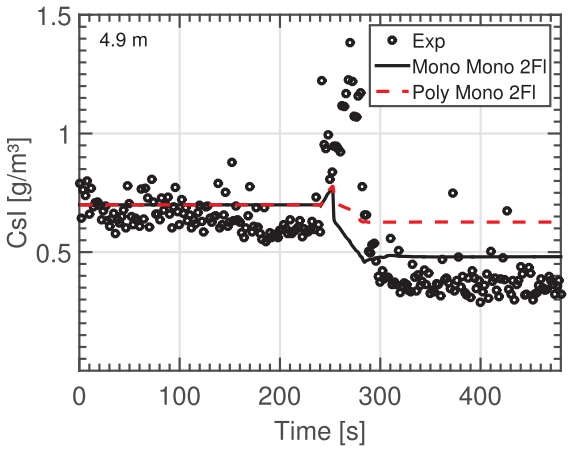

(a) Spray 1; 4.9 m

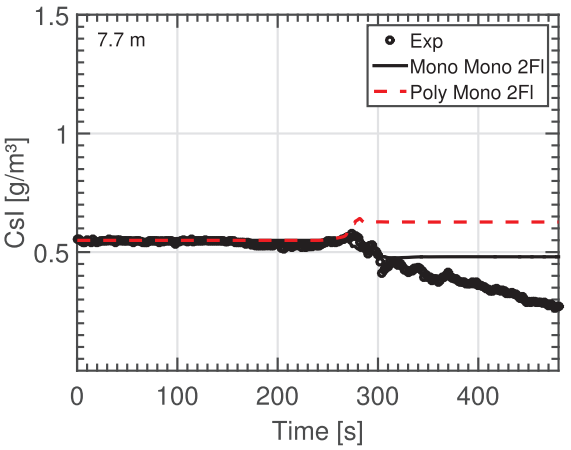

(b) Spray 1; 7.7 m

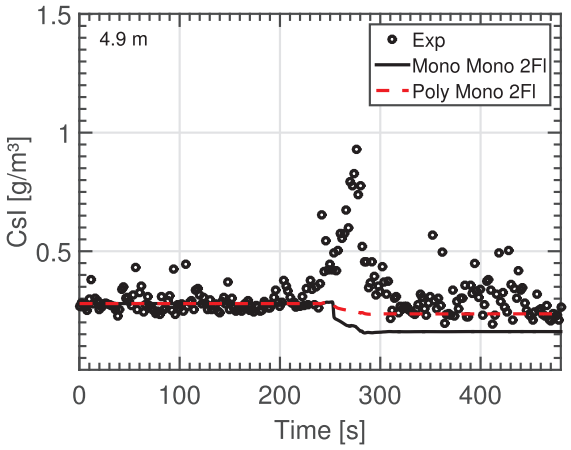

(c) Spray 2; 4.9 m

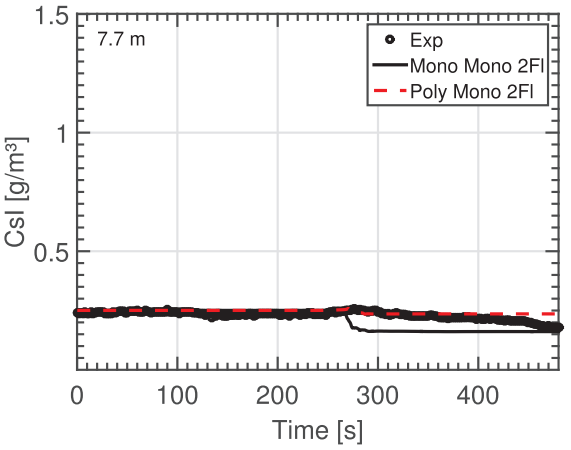

(d) Spray 2; 7.7 m

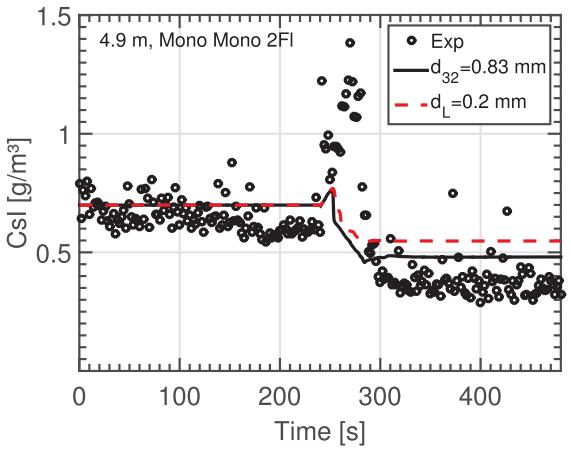

(e) Spray 1; 4.9 m droplet size comparison

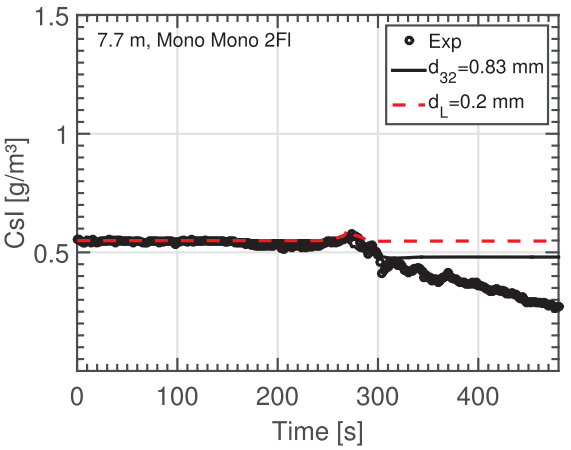

(f) Spray 1; 7.7 m droplet size comparison

Fig. 14. CsI concentration comparison of experiment and simulation (mono-/polydisperse) at measure planes 4.4 m and 7.7 m for spray 1 and spray 2.

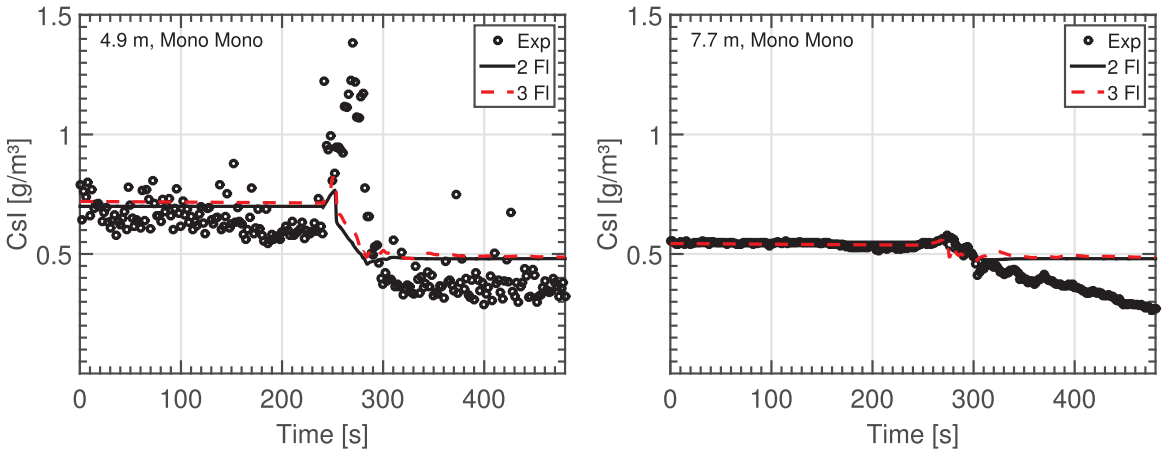

(a) Spray 1; 4.9 m (b) Spray 1; 7.7 m

Fig. 15. Comparison of two-fluid and three-fluid approach in spray 1.

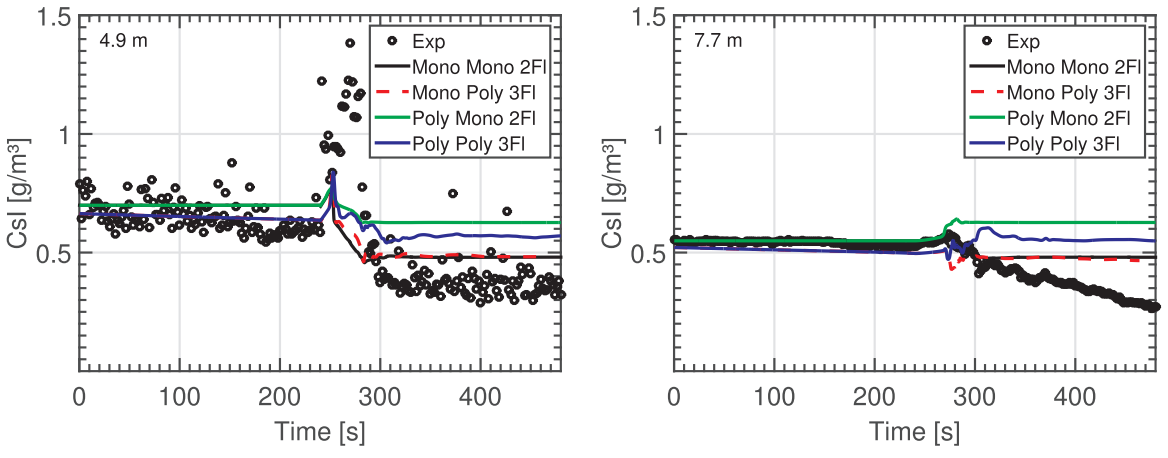

(a) Spray 1; 4.9 m (b) Spray 1; 7.7 m

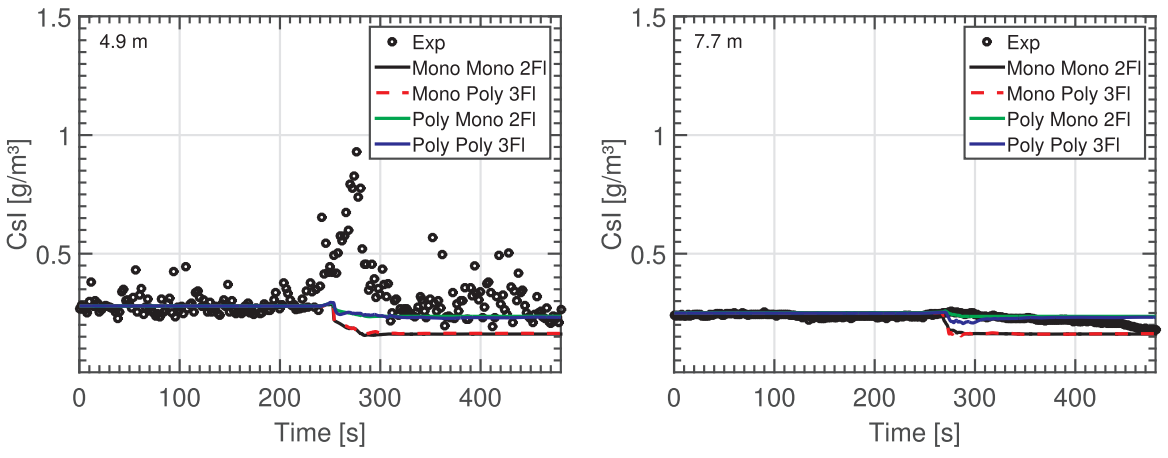

(c) Spray 2; 4.9 m (d) Spray 2; 7.7 m

Fig. 16. Comparison of two-fluid and three-fluid approach.

6.4. Comparison of mono- and polydisperse three-fluid approach in spray 1 and spray 2

In this section, simulations using a three-fluid approach with mono- and polydisperse droplet and aerosol particle distribution are presented (Mono Poly 3Fl, Poly Poly 3Fl). To point out the difference to the two-fluid approach, the simulations Mono Mono 2Fl and Poly Mono 2Fl are added in the plots, see Fig. 16.

The comparison in the graph for spray 1 shows a considerable disagreement between mono- and polydisperse spray configurations at both measure planes. The monodisperse spray configurations (Mono Mono 2Fl and Mono Poly 3Fl) present a more effective washout process than the polydisperse one. At a first glance, this is not expected, since the polydisperse spray configurations (Poly Mono 2Fl and Poly Poly 3Fl) model the reality more accurate. The phenomenon was already discussed in Section 6.2 for a polydisperse spray configuration using a two-fluid approach. Fig. 16 point out a small influence of particle distribution. The simulations Mono Poly 3FL and Poly Poly 3FL consider a spectrum for particles. The comparison for the monodisperse droplet simulations show a negligible small influence of a particle distribution. Both simulations calculate the same CsI content after spray injection. In the polydisperse spray configuration, particle distributions influence the washout efficiency. The spray configuration with polydisperse particles has a better agreement with the experiment at both measure planes compared to the monosized particle simulation. Smaller particles can be washed out by smaller droplets, whereas smaller droplets have less influence on larger monosized particles. When particles are modeled with a seperate flow field, the settling process in the first spray sequence until 240 s can be simulated very good. Due to gravity, particles accelerate towards the lower plenum and reduce the CsI content in the upper part. The deviation between the two-fluid and the three-fluid approach in the first spray sequence can be explained therefore by settling.

Spray 2 shows a far better agreement between experiment and polydisperse droplet configurations. Here, no difference in the CsI content after spray can be obtained, whether the particles are modeled monodisperse or with a spectrum. In spray 2, the monodisperse particle diameter is decreased to 1.19 μm and it seems, that the aerosol particle diameter is small enough that a spectrum can be neglected. In spray 2, the monodisperse droplet configuration overpredicts the aerosol particle removal rate. Due to the same droplet configuration used in spray 1 and smaller aerosol particles in spray 2, the removal rate is too efficient.

6.5. Mesh and timestep independence study

Results gained in CFD simulations are often influenced by the resolution of the flow field and the used time step. To investigate the grid effect in the presented simulations, the CsI content for three different meshes (see Table 1) at the measure planes 4.9 m and 7.7 m are plotted. The simulations for the mesh study is carried out with a monodisperse droplet and aerosol particle configuration using the two-fluid approach (Mono Mono 2Fl). Fig. 17 shows the comparison.

When the results for the three meshes are compared to each other, a negligible small difference in the CsI content during the spray part can be obtained and there is no impact on the CsI after the spray in the homogenization process. Due to the fact, that there is no relevant difference in the calculated data and from experience in previous work with THAI (e.g. Kaltenbach & Laurien, 2017), the mesh with eight million elements is used for the current investigations.

With the same simulation approach (Mono Mono 2Fl), the influence of different constant time steps was assessed. Fig. 18 presents the CsI content at the measure planes for three different time steps, namely 0.1 s, 0.15 s and 0.25 s. The graphs show no difference for the time steps 0.1 s and 0.15 s. The used time step .25 s and the corresponding results for the CsI content in the current publication has a small deviation to the smaller simulations, the results change only marginally. With this procedure, the simulation time could be nearly reduced by 50% when a time step of 0.25 s is used instead of 0.1 s. Time step assessment in addition to a mesh sensitivity study is always recommended for every transient simulation. Rarely the results of such investigations are universally valid.

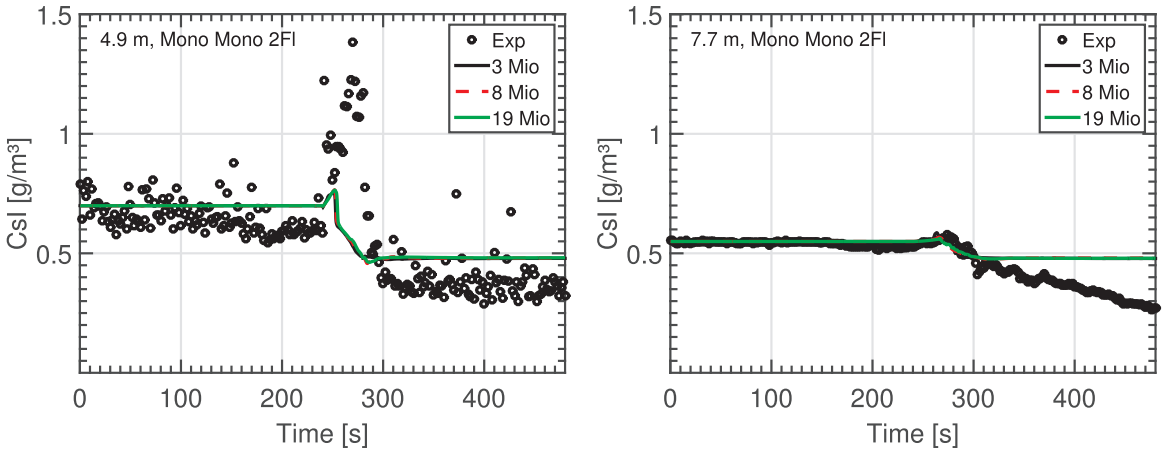

(a) Spray 1; 4.9 m (b) Spray 1; 7.7 m

Fig. 17. Study to investigate the mesh influence on simulation results.

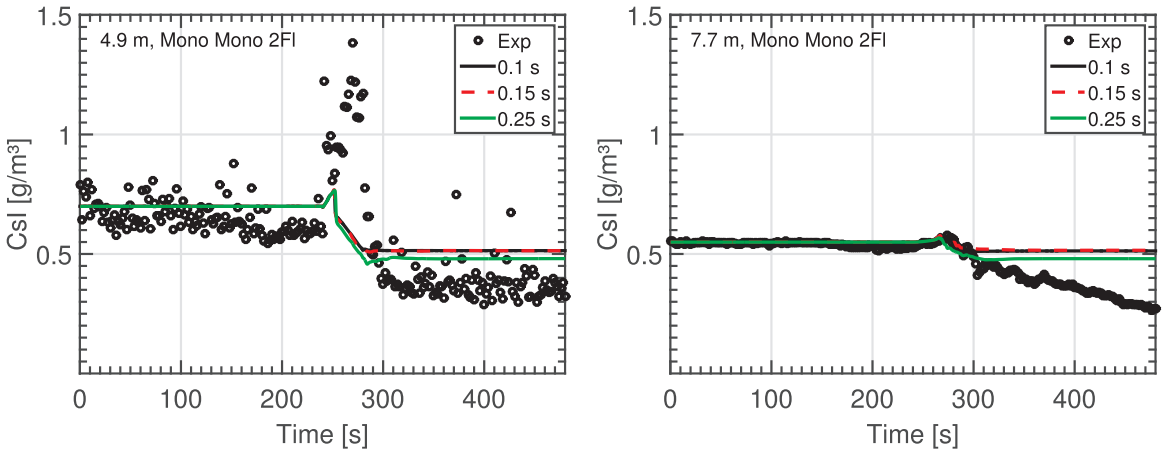

(a) Spray 1; 4.9 m (b) Spray 1; 7.7 m

Fig. 18. Study to investigate the time step influence on simulation results.

7. Conclusion

In the present paper, a physical model for the washout process of aerosol particles with water spray is presented. The model considers mechanical mechanisms like settling, inertial impaction, interception and Brownian diffusion and is implemented in the commerical CFD code ANSYS CFX via user-defined functions. The different washout mechanisms are described phenomenological and with appropriate correlations for the application in nuclear reactor safety. Validation is done with data from the experiment THAI AW4. The model is applied to an Euler-Euler two-fluid and for comparison to an Euler-Euler three-fluid approach. A mono- and polydisperse spray configuration is used as well as a mono- and polydisperse particle size distribution. The results show in detail a qualitative distribution of CsI in THAI before, during and after spray activation. Moreover the enrichment process of droplets with aerosol particles are shown graphically. A quantitative comparison between experiment and simulation is done on two measure planes at different heights for two spray transients, spray 1 and spray 2.

CFD simulations demand high qualitative validation experiments. Important for the simulations is a detailed knowledge of the droplet size distribution at the injection nozzle and the composition of the aerosol atmosphere with its particle distribution. Helpful for the validation process is an increasing amount of measure planes in the containment to improve the developed model more in detail.

Acknowledgements

This work is funded by the German Federal Ministry of Economic Affairs and Energy (BMWi) under grant number 1501493 on the basis of a decision by the German Bundestag. We gratefully acknowledge for using the Cray XC 40 (Hazel Hen) at the High-Performance Computing Center Stuttgart (HLRS) for the CFD simulations. Furthermore the authors would like to acknowledge Dr.-Ing. Martin Freitag (Becker Technologies GmbH) for providing the experimental data of THAI AW4, which was funded by BMWi under grant number 1501455.

References

Crowe, C., Sommerfeld, M., & Tsuji, Y. (1998). *Multiphase flows with droplets and particles.* Boca Raton, FL, USA: CRC-Press.

Gupta S., Langer, G., & Colombet, M. (2014). Hydrogen combustion during spray operation: Tests hd-30, hd-31 and hd-32.

Gupta, S., Schmidt, E., von Laufenberg, B., Freitag, M., Poss, G., Funke, F., & Weber, G. (2015). Thai test facility for experimental research on hydrogen and fission product behaviour in light water reactor containments. *Nuclear Engineering and Design, 294*, 183–201.

Ishii, M., & Hibiki, T. (2006). *Thermo-fluid dynamics of two-phase flow.* New York, NY, USA: Springer.

Ishii, M., & Mishima, K. (1984). Two-fluid model and hydrodynamic constitutive relations. *Nuclear Engineering and Design, 82*, 107–126.

Jung, C. H., & Lee, K. W. (1998). Filtration of fine particles by multiple liquid droplet and gas bubble systems. *Aerosol Science and Technology, 29*(*5*), 389–401.

Kaltenbach, C., & Laurien, E. (2017). Cfd simulation of aerosol removal by a spray in the model containment thai. In *Proceedings of the 17th International Topical Meeting on Nuclear Reactor Thermal Hydraulics (NURETH-17)*.

Kessler, G., Veser, A., Schlüter, F. -H., Raskob, W., Landman, C., & Päsler-Sauer, J. (2014). *The risks of nuclear energy technology. Safety concepts of light water reactors.* Berlin: Springer (GER).

Licht, W. (1980). *Air pollution control engineering: Basic calculations for particulate collection.* New York, NY, USA: Dekker.

Malet, J., & Huang, X. (2015). Influence of spray characteristics on local light gas mixing in nuclear containment reactor applications. *Computers & Fluids, 107*, 11–24.

Malet, J., Mimouni, S., Manzini, G., Xiao, J., Vyskocil, L., Siccama, N. B., & Huhtanen, R. (2015). Gas entrainment by one single french pwr spray, sarnet-2 spray benchmark. *Nuclear Engineering and Design, 282*, 44–53.

Marchand, D., Porcheron, E., Lemaitre, P., & Grehan, G. (2006). Characterization of the washout of aerosols by spraying water for thermal hydraulic conditions representative of a severe accident in nuclear reactor containment. In *Proceedings of International Conference on Liquid Atomization and Spray Systems (ICLASS)*.

Menter, F. (1994). Two-equation eddy-viscosity turbulence models for engineering applications. *American Institute of Aeronautics and Astronautics (AIAA), 32*(*32*).

Mimouni, S., Lamy, J.-S., Lavieville, J., Guieu, S., & Martin, M. (2010). Modelling of sprays in containment applications with a cmfd code. *Nuclear Engineering and*

Design, 240, 2260–2270.
Park, S. H., Jung, C. H., Jung, K. R., Lee, B. K., & Lee, K. W. (2005). Wet scrubbing of polydisperse aerosols by freely falling droplets. *Journal of Aerosol Science, 36*(12), 1444–1458.
Parsly, L. F. (1971). Removal of radioactive particles by spray.
Porcheron, E., & Lemaitre, P. (2008). Analysis of aerosol collection by droplets: Application to fission products removal in case of severe accident. In *Proceedings of the 16th International Conference on Nuclear Engineering (ICONE16)*.
Schmidt, E., Colombet, M., Freitag, M., Gupta, S., von Laufenberg, B. (2015). Aerosol spray test with csi aerosols.
Seinfeld, J., & Pandis, S. (2006). *Atmospheric chemistry and physics.* Hoboken, NJ, USA: Wiley.
Strauss, W. (1975). Industrial Gas Cleaning: (2nd Edition - S.I.Units). Pergamon Press, Sydney, AUS, 2 edition.